LONG-TERM EVOLUTION AND PHYSICAL PROPERTIES OF ROTATING RADIO TRANSIENTS

by

Ali Arda Gençali

Submitted to the Graduate School of Engineering and Natural Sciences
in partial fulfillment of
the requirements for the degree of
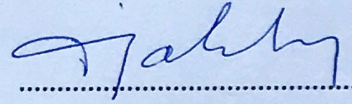Master of Science
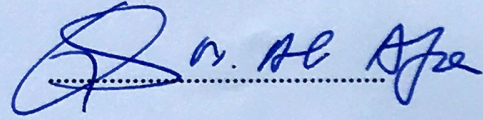
Sabancı University
June 2018

LONG-TERM EVOLUTION AND PHYSICAL PROPERTIES OF ROTATING RADIO TRANSIENTS

APPROVED BY
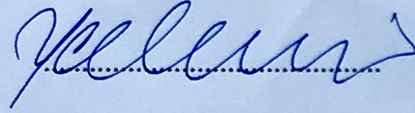
Assoc. Prof. Ünal Ertan   ....
(Thesis Supervisor)

Prof. Mehmet Ali Alpar   ....

Prof. Kazım Yavuz Ekşi   ....

DATE OF APPROVAL   27. 06. 2018

LONG-TERM EVOLUTION AND PHYSICAL PROPERTIES OF ROTATING RADIO TRANSIENTS

Ali Arda Gençali

Physics, Master of Science Thesis, 2018

Thesis Supervisor: Assoc. Prof. Ünal Ertan

Abstract

A series of detailed work on the long-term evolutions of young neutron star populations, namely anomalous X-ray pulsars (AXPs), soft gamma repeaters (SGRs), dim isolated neutron stars (XDINs), "high-magnetic-field" radio pulsars (HBRPs), and central compact objects (CCOs) showed that the X-ray luminosities, L_{X}, and the rotational properties of these systems can be reached by the neutron stars evolving with fallback discs and conventional dipole fields. Remarkably different individual source properties of these populations are reproduced in the same model as a result of the differences in their initial conditions, magnetic moment, initial rotational period, and the disc properties. In this thesis, we have analysed the properties of the rotating radio transients (RRATs) in the same model. We investigated the long-term evolution of J1819–1458, which is the only RRAT detected in X-rays. The period, period derivative and X-ray luminosity of J1819–1458 can be reproduced simultaneously with a magnetic dipole field strength $B_0 \sim 5 \times 10^{11}$ G on the pole of the neutron star, which is much smaller than the field strength inferred from the dipole-torque formula. Reasonable model curves are obtained with disc masses in the range of $(0.75 - 3.76) \times 10^{-5}\ M_\odot$, producing the source properties, in the accretion phase at ages $\sim 2 \times 10^5$ yr. Our results are not sensitive to the initial period. We find that J1819–1458 is close to and below the radio pulsar death line with this B_0 and the measured period. The numerical simulations indicate that J1819–1458 is evolving toward the properties of XDINs, which implies that there is a close evolutionary connection between RRATs and XDINs. For 29 RRATs with measured period derivatives and unknown X-ray luminosities, we estimate the minimum B_0 values in the fallback disc model. These lower limits on the field strengths are sufficiently low such that the actual dipole fields of RRATs could fill the B_0 gap between XDINs and CCOs in this model. Finally, we discuss the possible evolutionary links between RRATs and the other young neutron star populations.

GEÇİCİ DÖNEN RADYO KAYNAKLARININ UZUN SÜRELİ EVRİMLERİ VE FİZİKSEL ÖZELLİKLERİ

Ali Arda Gençali

Fizik, Yüksek Lisans Tezi, 2018

Tez Danışmanı: Doç. Dr. Ünal Ertan

Özet

Anormal X-ışını kaynakları (AXPs), gama ışını tekrarlayıcıları (SGRs), sönük izole kaynaklar (XDINs), "yüksek manyetik alanlı" radyo pulsarları (HBRPs) ve merkezi yoğun cisimler (CCOs) genç nötron yıldız popülasyonlarıdır ve bu popülasyonların uzun dönem evrimleri üzerine yapılan bir dizi detaylı çalışma gösterdi ki kalıntı diski ve klasik dipol alanıyla evrilen nötron yıldızları, bu sayılan sistemlerin X-ışını ışıma gücü, L_{X}, ve dönme özelliklerine ulaşabilirler. Başlangıç koşulları, manyetik momenti, başlangıç dönme periyodu ve disk özelliklerindeki farklılıkların neticesinde bu popülasyonların dikkat çekecek biçimde farklı tekil kaynak özellikleri aynı model kullanılarak tekrar üretilirler. Bu tezde, biz geçici dönen radyo kaynaklarının (RRATs) özelliklerini aynı model çerçevesinde analiz ettik. Biz X-ışınında saptanmış tek RRAT olan J1819–1458' in uzun dönem evrimini inceledik. Nötron yıldızının kutubundaki manyetik dipol alan gücünü $B_0 \sim 5 \times 10^{11}$ G alarak, J1819–1458' in periyot, periyot türevi ve X-ışını ışıma gücü eşzamanlı olarak tekrar üretilebilmektedir, bu alan gücü dipol-tork fomülü kullanılarak elde edilenden daha düşüktür. Farklı disk kütleleri $(0.75 - 3.76) \times 10^{-5} \ M_\odot$ aralığında alındığında, makul model eğrileri kaynak özelliklerini üretecek şekilde yaklaşık olarak 2×10^5 yaşında ve kütle aktarım fazında saptanmaktadır. Bizim sonuçlarımız başlangıç periyotlarına hassas değildir. Biz J1819–1458' u saptanmış B_0 değeri ve ölçülmüş periyoduyla radyo pulsar ölüm çizgisine yakın ve altında bulduk. Nümerik simülasyonlar gösterdi ki J1819–1458 XDIN' lerin özelliklerine doğru evrilmektedir ve bu durum RRAT' lar ile XDIN' ler arasında yakın bir evrimsel bağ olduğunun işaretidir. Ölçülmüş periyot türevi ve bilinmeyen X-ışın güçlerine sahip 29 RRAT için kalıntı diski modelini kullanarak minimum B_0 değerlerini tahmin ettik. Bu alan güçleri üzerindeki alt limitler yeterince düşüktür, öyle ki RRAT' ların gerçek dipol alanları XDIN' ler ile CCO' lar arasındaki B_0 boşluğunu bu

modelde doldurabilir. Son olarak, RRAT' lar ile diğer genç nötron yıldızı popülasyonları arasındaki olası evrimsel bağlantılar tartışıldı.

ACKNOWLEDGEMENTS

Contents

List of Figures

LIST OF ABBREVIATIONS

AXP	Anomalous X-ray Pulsars
SGR	Soft Gamma Repeater
XDIN	Dim Isolated Neutron Star
HBRP	High Magnetic Field Radio Pulsar
CCO	Central Compact Object
RRAT	Rotation Radio Transient
LMXB	Low Mass X-ray Binary
HMXB	High Mass X-ray Binary

Chapter 1

INTRODUCTION

1.1   Neutron Stars

When thermo-nuclear reactions terminate at the core of a massive main-sequence star, thermal pressure cannot support the star against gravity. Subsequently, the core of the star collapses in a short time, producing a very strong explosion, a "supernova", ejecting the outer layers of the star. A supernova is estimated to produce either a neutron star or a black hole depending on the mass of the main-sequence star. During the collapse, if the gravitational force is balanced by the neutron degeneracy pressure, the core becomes a neutron star. A typical neutron star has a mass close to one solar mass, $M_\odot = 1.99 \times 10^{33}$ g, confined within a radius of 10 km, which corresponds to an enormous mean density of $\sim 10^{15}$ g cm^{-3}. Due to the conservation of angular momentum and magnetic flux through the core during the collapse, neutron stars are born with extremely high rotation rates and strong magnetic dipole fields. A newly born neutron star can reach a rotational period, P, as short as milliseconds, and a magnetic dipole field strength greater than $\sim 10^{12}$ G on the surface of the star. If the mass of the core is above a critical value ($\sim 3~M_\odot$), even the neutron-degeneracy pressure is not sufficient to balance the gravity of the star, and the core continues to collapse, eventually producing a black hole.

Two years after the discovery of the neutron by Chadwick (1932), it was proposed that neutron stars could exist (Baade & Zwicky, 1934). They suggested that supernova explosions could produce compact objects that are much denser than white dwarfs, and supported by neutron-degeneracy pressure against gravity. Even before the discovery of neutrons, Landau had speculated that compact objects denser than white dwarfs could exist. Later, Oppenheimer & Volkoff (1939) and Tolman (1939) independently estimated that the mass of a neutron star is less than about $0.7~M_\odot$ neglecting nucleon-nucleon

interactions. Later, including these interactions in the calculations, the maximum mass of a neutron star was estimated to be $\sim 2\ M_\odot$ (Cameron, 1959).

Pacini (1967) showed that a rapidly rotating neutron star with a strong magnetic dipole field creates strong electric fields that accelerate charged particles and produce electromagnetic radiation. Gold (1968) suggested that these neutron stars have strong magnetic fields $\sim 10^{12}$ G, and should be slowing down by magnetic dipole radiation at the expense of their rotational energies. According to the standard model (light-house model), beams of radio waves are produced by the charged particles (electrons and positrons) accelerated along the open field lines originating from the magnetic poles of the neutron star. There is an angle, α, between rotational and magnetic axes of a neutron star (see Figure 1.1). The radio emission is emitted within a conic solid angle as seen in Figure 1.1. If this radio beam sweeps the position of the observer during the rotation of the star, the observer receives a radio pulse per rotation period of the neutron star. Some sources could show two pulsations in one rotation period, depending on the viewing geometry, beaming angle and the angle between the rotation and magnetic axes. Many radio pulsars also emit pulsed radiation at other wavelengths of the electromagnetic spectrum from optical to gamma-rays.

The first radio pulsar was discovered by a PhD student Jocelyn Bell and her supervisor Anthony Hewish. The source (PSR 1919+21) was regularly pulsating radio waves with a period $P = 1.377$ s (Hewish et al., 1968). Later, many radio pulsars with much shorter periods were detected. These very regular pulsations with such short periods indicated that these sources should be rapidly rotating neutron stars, because gravitational forces of white dwarfs, which have masses comparable to $M_\odot$, and radii ($\sim 10^9$ cm) three orders of magnitude greater than these of neutron stars, cannot support these rapid rotations. At present, there are more than 2500 radio pulsars that have been detected in the last 50 years. Among these radio pulsars, the shortest period is 1.4 ms (Hessels et al., 2006), and the longest period is 8 s (Young, Manchester & Johnston, 1999). Their period derivatives, $\dot{P}$, vary from $\sim 10^{-20}$ s s^{-1} to $\sim 10^{-12}$ s s^{-1} (see Figure 1.2).

Due to compactness of neutron stars, mass-flow onto these objects is a very powerful electromagnetic radiation mechanism, more efficient than even fusion reactions. Neutron stars and black holes in close binary systems could accrete matter from their companions. The matter flowing onto the surface of a neutron star produces electromagnetic radiation

emitted mostly in X-rays. The accretion luminosity can be written as $L_{\mathrm{X}} = GM_* \dot{M}/R$, where R and M_* are the radius and the mass of the neutron star, $\dot{M}$ is the rate of mass accretion onto the neutron star and G is the gravitational constant (Davidson & Ostriker, 1973).
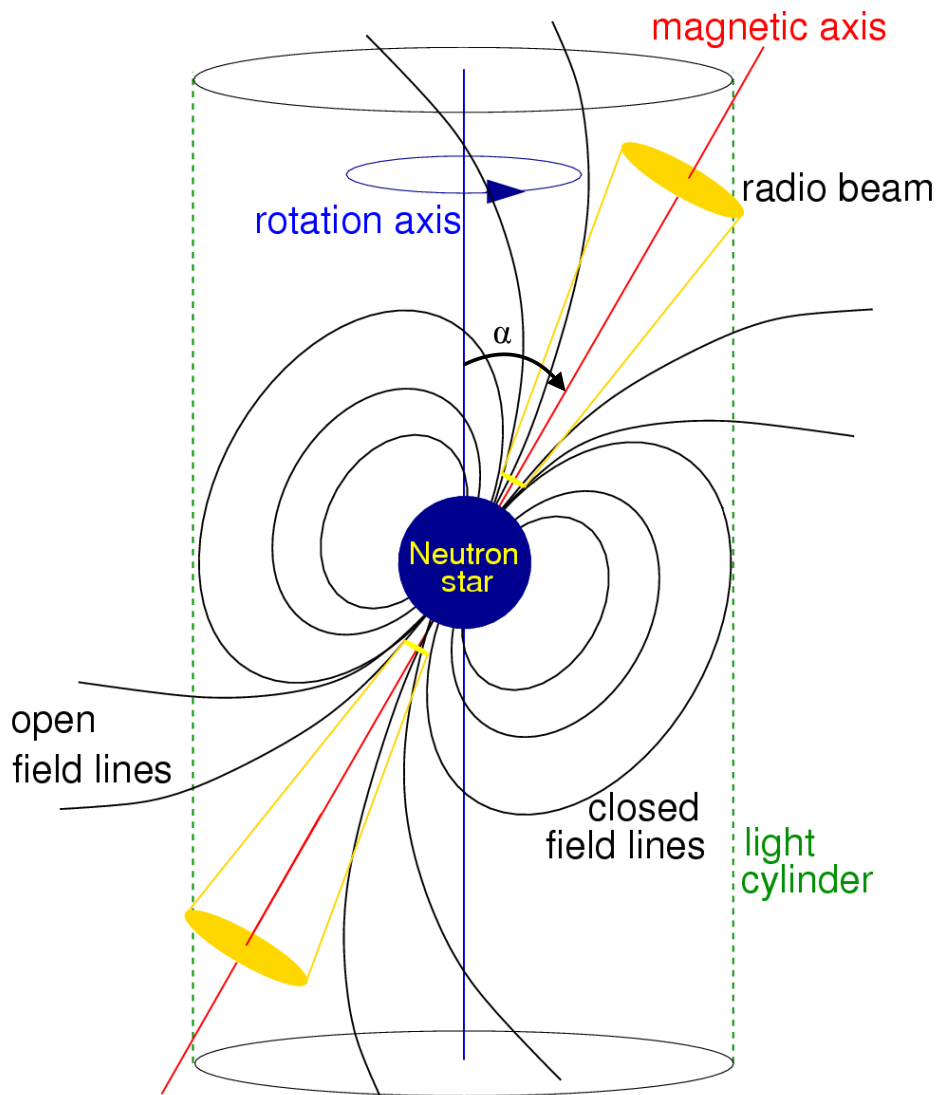
Figure 1.1: A simplified picture of a radio pulsar. In the figure α is the angle between the rotational axis and the magnetic field axis. Outside the light cylinder radius the magnetic field lines are open. Radio beams are emitted from the polar cap along the open field lines as shown in the figure. The radio beams traces a certain portion of the sky as the neutron star rotates around the rotation axis. This figure was taken from the Handbook of Pulsar Astronomy by Lorimer and Kramer and modified.
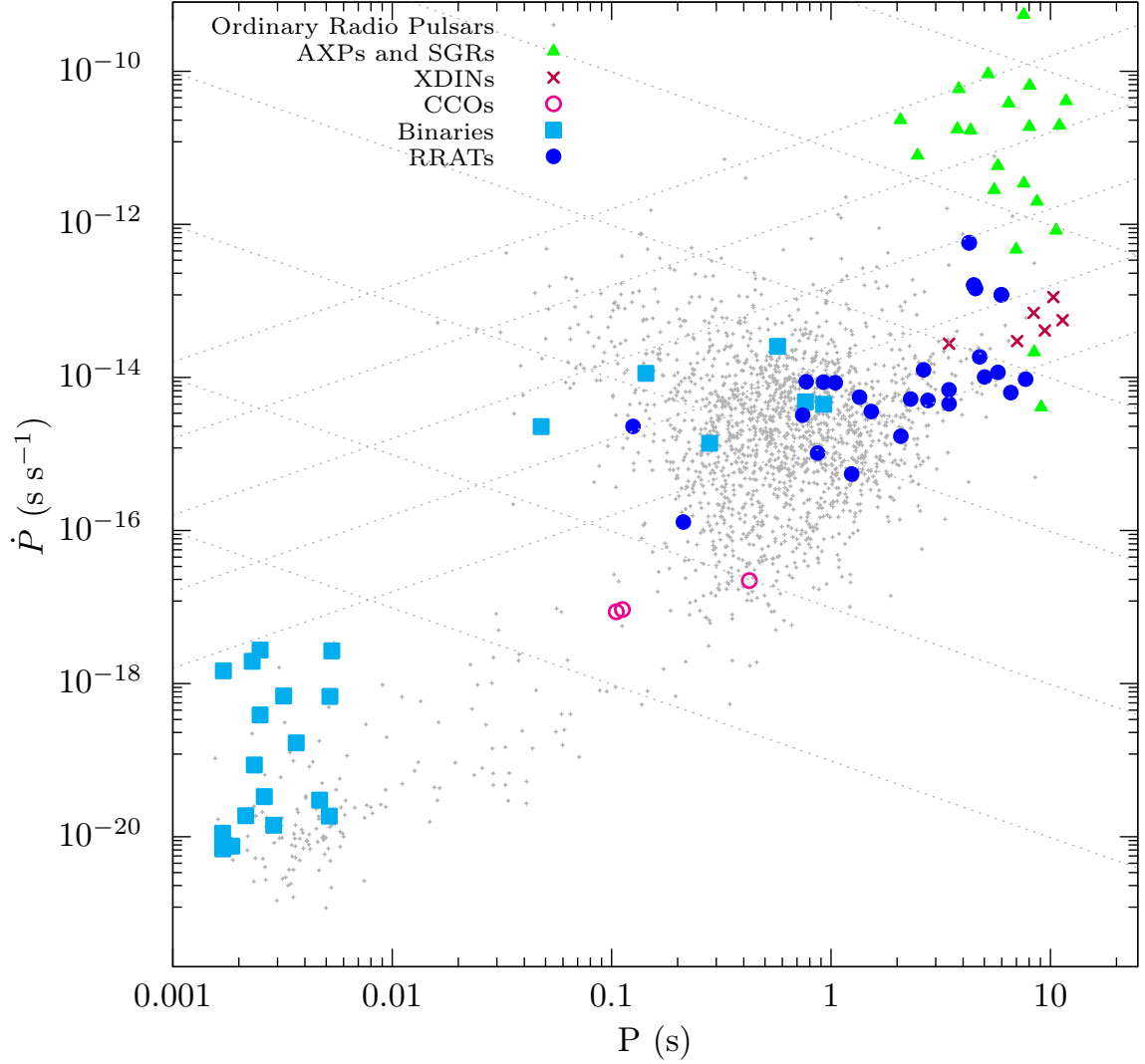
Figure 1.2: $P - \dot{P}$ diagram of the single neutron star populations and the millisecond pulsars recycled in binaries (from `http://www.atnf.csiro.au/people/pulsar/psrcat/`).

Most of the main-sequence stars are in binary systems. In these systems, one of the stars with higher mass evolves more rapidly and could become a compact star. If the supernova does not disrupt the binary system, subsequent evolution of the normal star (companion) could lead to mass flow onto the primary (compact star), and produce an X-ray binary. The mass transfer from the companion could be by means of wind accretion, if the mass of the companion is greater than several $M_\odot$ (Bondi & Hoyle, 1944; van den Heuvel & Heise, 1972). These systems are called high-mass X-ray binaries (HMXBs). If the secondary is a low-mass star ($M \lesssim M_\odot$), the mass-flow is likely to be through Roche-lobe overflow that could lead to formation of an accretion disc around the compact object, which is possible for sufficiently close binary stars. These systems are called low-

mass X-ray binaries (LMXBs). The compact star in a LMXB could be a neutron star or a black hole.

The rotational periods of neutron stars in HMXBs are in the range of $60 - 850$ s (see White, 2002, and references therein), while the periods of neutron stars in LMXBs are measured to be a few milliseconds. Estimated surface magnetic dipole field strengths of neutron stars are $\sim 10^{12}$ G in HMXBs (Bhalerao et al., 2015) and $\sim 10^8 - 10^9$ G in LMXBs (Burderi, King & Wynn, 1996; Burderi & D'Amico, 1997), indicating that HMXBs are much younger than LMXBs, and the weak fields of the neutron stars in LMXBs are likely to be resulting from the field decay during the long-term evolution of these sources (Srinivasan et al., 1990; Ding, Cheng & Chau, 1993; Jahan Miri & Bhattacharya, 1994; Konar & Bhattacharya, 1997, 1999; Ruderman, Zhu & Chen, 1998). The millisecond periods of the old neutron stars in LMXBs could be achieved by the spin-up torques provided by the matter accreting onto the neutron star in the long-term evolution of the system (Alpar et al., 1982; Radhakrishnan & Srinivasan, 1982).

During the evolution of LMXBs, when the companion star fills its Roche-lobe, the gas flows from the Roche-lobe of the companion to that of the neutron star from the inner Lagrangian point, L_1 (Lewin, van Paradijs & van den Heuvel, 1995). Since the matter enters the Roche-lobe of the neutron star with a large angular momentum, it cannot flow directly onto the surface of the neutron star. Instead, conservation of angular momentum and the gravity of the neutron star lead to formation of a geometrically thin accretion disc around the star (Pringle & Rees, 1972). In the accretion disc, the matter moves with Kepler velocity in the orbital (ϕ) direction interacting with the matter at neighbor radii. Along the disc, turbulent viscous interactions transfer angular momentum outwards, while the matter flows inwards (Shakura & Sunyaev, 1973). In a steady state, the rate of mass-flow from the companion becomes equal to the accretion rate onto the neutron star.

The first X-ray source, SCO X-1, was detected during the rocket experiments by Giacconi et al. (1962) before the discovery of radio pulsars. Shklovsky (1967) suggested that this bright source could be an accreting neutron star in a binary system. Almost one decade ago SCO X-1 was accepted as a member of LMXBs with new observations. Later, in 1971, UHURU satellite detected other pulsating X-ray sources powered by accretion in binary systems. One of the first observed source with UHURU was Cen X-3 which is a HMXB.

In the last two or three decades, with developing observational techniques at all electromagnetic wavelengths, new isolated neutron star populations were discovered with properties different from ordinary radio pulsars (see Pavlov et al., 2001; Abdo et al., 2013, and references therein). These populations, namely dim isolated neutron stars (XDINs), anomalous X-ray pulsars (AXP), soft gamma repeaters (SGRs), so called "high-magnetic-field" radio pulsars (HBRPs), central compact objects (CCOs) and rotating radio transients (RRATs), show both similarities and striking differences. For instance, the periods of AXP/SGRs and XDINs are all clustered to a narrow range of $2 - 12$ s. Rotation of all these young neutron star populations are slowing down. Repeating short and energetic soft gamma-ray bursts, that were initially observed only from SGRs (Mazets, Golenetskij & Guryan, 1979; Mazets et al., 1979), have been detected later from AXPs (Kaspi et al., 2003; Israel et al., 2007) and HBRPs as well. The magnetic dipole field strengths inferred from the measured P and $\dot{P}$ values of these sources with the purely dipole torque assumption range from $\sim 10^{10}$ G (for CCOs) to greater than 10^{14} G (for AXP/SGRs).

In addition to sporadic and super-Eddington soft gamma-ray bursts of AXPs and SGRs, three SGRs showed giant flares with luminosities $L \geq 10^{44}$ erg s^{-1} (Mazets, Golenetskij & Guryan, 1979; Hurley et al., 1999; Palmer et al., 2005). AXP/SGRs show X-ray pulsations with periods in the $2 - 12$ s range and period derivatives $\sim 10^{-13} - 10^{-10}$ s s^{-1} (Olausen & Kaspi, 2014). The estimated characteristic ages of AXP/SGRs vary between ~ 100 yr and 10^7 yr. Persistent X-ray luminosities ($10^{33} - 10^{36}$ erg s^{-1}) of most of these sources are well above their rotational powers, $\dot{E} = I\Omega\dot{\Omega} \simeq 10^{32}$ erg s^{-1}, where I, Ω and $\dot{\Omega}$ are the moment of inertia, the angular frequency and the angular frequency derivative of the neutron star. Majority of the AXP/SGRs haven't been detected in the radio band. Only four sources show radio pulsations with properties rather different from those of ordinary radio pulsars (Mereghetti, 2013). Association of some AXP/SGRs with supernova remnants indicate that these are young objects. What is the source of their X-ray luminosity, and what is the torque mechanism that slows down these systems?

In the magnetar model (Duncan & Thompson, 1992; Thompson & Duncan, 1995), AXP/SGRs (and other young neutron star populations) are neutron stars rotating in vacuum, and slow down by purely magnetic dipole torques. With this assumption, the dipole field strength on the pole of the star is estimated from the dipole torque formula which gives $B_{\mathrm{d}} \approx 6.4 \times 10^{19} (P\dot{P})^{1/2} \gtrsim 10^{14}$ G for most of these systems. In this model,

it is proposed that the crust of the star could be heated continuously by field decay and produces the observed L_X. Hereafter, we use "B_d" and "B_0" to denote the dipole field strength on the pole of the star inferred from the dipole torque formula and estimated in our model respectively.

Both the source of X-ray luminosity and the torque mechanism are rather different in the fallback disc model (Chatterjee, Hernquist & Narayan, 2000; Alpar, 2001). In the presence of fallback discs that are estimated to have formed after the supernova (Colgate, 1971; Chevalier, 1989; Michel & Dessler, 1981), the dipole field strength deduced using the dipole torque overestimates the actual field strength by one or two orders of magnitude, because the magnetic torque originating from disc-field interaction dominates the magnetic dipole torque in most cases. In the fallback disc model, L_X is produced either by mass accretion onto the neutron star or by intrinsic cooling of the star when the system is in the propeller phase.

It was shown that the long-term evolution of neutron stars with fallback discs can explain the characteristic rotational and L_X properties of AXP/SGRs (Ertan et al., 2009). This model was later developed including the cooling luminosity of the neutron star, and its contribution to the X-ray heating of the disc, and the inactivation of the disc at low temperatures in the evolution of the neutron star (Ertan et al., 2009; Alpar, Ertan & Çalışkan, 2011; Çalışkan et al., 2013). This model can reproduce the individual properties of AXP/SGRs self-consistently (producing P, $\dot{P}$ and L_X simultaneously) only with $B_0 \sim 10^{12} - 10^{13}$ G. In other words, a hybrid model with a magnetar dipole field ($B_0 > 10^{14}$ G) and a fallback disc cannot account for the AXP/SGR properties (Alpar, 2001; Ekşi & Alpar, 2003; Ertan et al., 2007, 2009).

The short time-scales and energetics of SGR bursts require magnetar fields. As suggested by Ekşi & Alpar (2003), much earlier than the discovery of the so-called low-B magnetars (Livingstone et al., 2011; Rea et al., 2012), these strong fields could be stored in the small-scale multipoles, localized close to the star's surface, while the dipole component has conventional strength. Since the disc interacts with large-scale dipole component of the field, presence of magnetar quadrupoles is compatible with the fallback disc model. This indicates that SGR bursts do not necessitate magnetar dipole fields, which was confirmed by the discovery of the low-B magnetars with $B_d < 10^{13}$ G which showed typical SGR bursts (Livingstone et al., 2011; Rea et al., 2012). Furthermore, the same long-

term evolution model can explain the properties of low-B magnetars as well without any additional assumptions in the model (Benli et al., 2013).

The periods of XDINs are in the range of $3-11$ s like those of AXP/SGRs. The period derivatives are between 10^{-14} s s^{-1} and 10^{-13} s s^{-1}. From the dipole torque formula, $B_{\rm d}$ values for XDINs are estimated in the range of $10^{13}-10^{14}$ G. Their characteristic ages are estimated to be $\sim (1-4) \times 10^{6}$ yr which are greater than their estimated kinematic and cooling ages ($\sim 10^{5}-10^{6}$ yr). Measured X-ray luminosities of XDINs ($10^{31}-10^{32}$ erg s^{-1}) are greater than their $\dot{E} \sim 10^{30}-10^{31}$ erg s^{-1}. It is likely that $L_{\rm X}$ of XDINs are powered by intrinsic cooling of the neutron star. The difference in the temperatures at the polar and the equatorial regions could be the reason for the observed pulsed X-ray emission. Due to these low X-ray luminosities, XDINs are hard to be detected at large distances. All seven known XDINs are located ~ 500 pc. No pulsed radio emission has been detected from these sources (Haberl et al., 1997; Turolla, 2009). Non-detection of radio pulsations could be due to narrow beaming angles estimated for long-period systems. Or, their rotational rates and magnetic dipole moments are not sufficient to produce pulsed radio emission. A neutron star evolving with a fallback disc can reach the rotational properties and X-ray luminosites of XDINs with $B_{0} \sim 10^{11}-10^{12}$ G (Ertan et al., 2014; Ertan, 2017). The main disc parameters employed in this model are similar to those used for AXP/SGRs. The model results show that XDINs are currently in the propeller phase, and their $L_{\rm X}$ are powered by the cooling luminosity of the neutron star. The ages of the sources estimated in the model are close to their cooling and kinematic ages. The periods together with the estimated B_{0} values place XDINs below the pulsar death line in $B_{0}-P$ plane (Ertan et al., 2014, Fig. 4). That is, our model results imply that the non-detection of radio pulses from 6 of the currently known XDINs is not due to beaming affect.

HBRPs are radio pulsars which have relatively high $\dot{P}$ values ($10^{-14}-10^{-12}$ s s^{-1}) compared to those of ordinary radio pulsars. The rotational spin period of HBRPs are in the $0.1-7.7$ s range. For HBRPs, $B_{\rm d}$ estimated from the dipole torque formula, is $\sim 10^{13}-10^{14}$ G. The typical SGR bursts were also detected from the HBRPs (Gavriil et al., 2008; Younes, Kouveliotou & Roberts, 2016) indicating that there could be evolutionary links between HBRPs and AXP/SGRs (Keane & Kramer, 2008; Kaspi, 2010). The X-ray luminosities of HBRPs are in $10^{32}-10^{35}$ erg s^{-1} range while $\dot{E} \sim 10^{30}-10^{37}$ erg s^{-1}, and

the rotational power of these sources are generally greater than their L_X. The rotational properties and observed X-ray luminosities of HBRPs can be explained in the fallback disc model with $B_0 \sim 10^{12} - 10^{13}$ G, similar to the B_0-range of AXP/SGRs in the same model (Benli & Ertan, 2016, 2017, 2018b). The model sources are found to be evolving in the propeller phase at present, which is consistent with their radio pulsar properties. The ages estimated in the model in agreement with the estimated supernova ages of the sources.

CCOs are located close to the center of supernova remnants (SNR), hence CCOs are considerably younger than the other single neutron star populations. Currently, there are 10 confirmed CCOs. The period and period derivatives, that were measured for three sources, are in the ranges of $0.1 - 0.4$ s and $10^{-18} - 10^{-17}$ s s^{-1} (Gotthelf, Halpern & Alford, 2013). For CCOs, the dipole-torque formula gives $B_d \sim 10^{10}$ G much smaller than those of AXP/SGRs, XDINS and HBRPs. Like AXP/SGRs and XDINs, the X-ray luminosities of these sources ($\sim 10^{33}$ erg s^{-1}) (Gotthelf, Halpern & Alford, 2013) are also greater than their rotational powers ($\dot{E} \sim 10^{31} - 10^{32}$ erg s^{-1}). Observed X-ray spectra of CCOs can be fitted with two blackbodies with temperatures of 0.30 keV and 0.52 keV with emitting areas much smaller than the surface area of the neutron star (Halpern & Gotthelf, 2010). CCOs haven't been detected in the optical, infrared and radio bands yet. The characteristic ages of CCOs ($\tau_c \sim 10^8$ yr) are much grater than their estimated supernova ages ($\tau_{SN} \sim$ several kyr). Recently, Benli & Ertan (2018a) showed that CCO properties can be explained in the fallback disc model consistently with the estimated supernova ages. The estimated B_0 values for the three CCOs are a few 10^9 G (Benli & Ertan, 2018a), the weakest magnetic dipole fields among the young, single neutron star systems in the fallback disc model.

These results show that the long-term evolution of different young neutron star populations can be explained in the same fallback disc model with similar main disc parameters. Rather different individual source properties can be reproduced with dipole field strengths between $\sim$ a few 10^9 and 10^{13} G, which remain far below the B_d values inferred from the dipole torque formula. The distribution of these young neutron star populations in $P - \dot{P}$ diagram imply that there could be evolutionary links between these systems and RRAT population. It seems that there is a gap between the estimated dipole field strengths of CCOs ($B_0 \sim$ a few 10^9 G) and XDINs ($B_0 \gtrsim 10^{11}$), which could be filled with the B_0

distribution of RRAT population.

In this thesis, we concentrate on the long-term evolution and the physical properties of J1819–1458. We also estimated the minimum dipole field strengths of the other RRATs with known P and $\dot{P}$ values. Since these sources were not detected in the X-rays, detailed analysis of their evolutions is not possible. With this currently limited $L_{\rm X}$ information, we also try to understand the physical conditions responsible for the sporadic radio bursts of RRATs.

In Chapter 2, we investigate the long-term evolution of the RRATs with fallback discs, and summarize the details of the fallback disc model, and give the results of the model calculations for RRAT J1819–1458. In Chapter 3, we summarize the properties of all young neutron star populations obtained in the same model, and discuss their possible evolutionary links with RRATs.

Chapter 2

ROTATING RADIO TRANSIENT J1819–1458

Ali Arda Gençali, Ünal Ertan

2.1 Introduction

Rotating Radio Transients (RRATs) were discovered more than a decade ago as a new neutron star population (McLaughlin et al., 2006). Unlike normal radio pulsars, RRATs do not exhibit regular radio pulses. They show sporadic and brief radio bursts with time separations of $\sim$ minutes to a few hours. Durations of the radio bursts range from 0.5 ms to 100 ms with flux densities from ~ 10 mJy to ~ 10 Jy, which make these systems the brightest radio sources in the universe (McLaughlin et al., 2006; Deneva et al., 2009). Detectable radio emission from a particular RRAT lasts for less than one second per day (McLaughlin et al., 2006). From the analysis of burst times-of-arrival (Manchester et al., 2001), the rotational periods have been obtained in the $0.1 - 7$ s range (McLaughlin et al., 2006; Deneva et al., 2009). Among more than 100 confirmed RRATs (Taylor et al., 2016), only J1819–1458 was detected in X-rays (McLaughlin et al., 2007), and upper limits on the X-ray luminosity were estimated for J0847-4316 and J1846-0257 (Kaplan et al., 2009). The main reason for non-detection of the other RRATs in X-rays is the uncertainties in the positions of the sources (Kaplan et al., 2009).

For J1819–1458 (hereafter J1819), the rotational period $P = 4.26$ s (McLaughlin et al., 2006) and the period derivative $\dot{P} \approx 5.75 \times 10^{-13}$ s s^{-1} (Keane et al., 2011) give the characteristic age $\tau_\mathrm{c} = P/2\dot{P} \simeq 1.2 \times 10^5$ yr and the rotational power $\dot{E} \simeq 4\pi^2 I \dot{P} P^{-3} \simeq 3 \times 10^{32}$ erg s^{-1}, where I is the moment of inertia of the neutron star. Radio bursts from J1819, repeating about every four minutes, were detected in Parkers observations (McLaughlin et al., 2006). The distance is estimated to be $d = 3.6$ kpc from the dispersion measure with an uncertainty of $\sim 25\%$ (McLaughlin et al., 2006). An unabsorbed flux of 1.5×10^{-13} erg s^{-1} cm^{-2} detected in the $0.3 - 5$ keV band gives an X-ray luminosity $L_\mathrm{x} = 4 \times 10^{33} \, (d/3.6 \text{ kpc})^2$ erg s^{-1}, which is an order of magnitude higher than the rotational power of the source (Rea et al., 2009).

The reason for the transient nature of the radio emission from RRATs has not been understood yet. It was proposed that RRATs could have properties similar to the systems that show giant pulses (Knight et al., 2006) or to nulling pulsars (Redman & Rankin, 2009). Alternatively, RRATs could be the radio pulsars close to the pulsar death line in the magnetic dipole field-period plane (Chen & Ruderman, 1993). In this late phase of radio-pulsar evolution, pulsations might become rare (Zhang, Gil & Dyks, 2007). These

systems might be emitting weak, continuous radio pulses, which have not been detected yet, in addition to the observed short radio bursts (Weltevrede et al., 2006). It was also proposed that RRATs could have evolutionary links with the anomalous X-ray pulsars (AXPs), soft gamma repeaters (SGRs) (McLaughlin et al., 2006, 2009) or thermally emitting dim isolated neutron stars (XDINs) (Popov, Turolla & Possenti, 2006). This possibility has motivated us to study the long-term evolution of J1819 in the fallback disc model that was applied earlier to the other neutron star populations.

The fallback disc model was first proposed to explain the long-term X-ray luminosity and period evolution of AXPs (Chatterjee, Hernquist & Narayan, 2000). It was proposed by Alpar (2001) that the observed properties of not only AXPs but also other neutron star populations, SGRs, XDINs, and possibly central compact objects (CCOs), could be explained if the fallback disc properties are included in the initial conditions in addition to the magnetic dipole moment and the initial period. To test these ideas, a long-term evolution model for neutron stars with fallback discs was developed including the effects of X-ray irradiation with contribution of the intrinsic cooling of the neutron star, and the inactivation of the disc at low temperatures on the evolution of the star (Ertan et al., 2009; Alpar, Ertan & Çalışkan, 2011; Çalışkan et al., 2013). Later, it was shown that the individual source properties of AXP/SGRs (Benli & Ertan, 2016), XDINs (Ertan et al., 2014), high magnetic-field radio pulsars (HBRPs) (Çalışkan et al., 2013; Benli & Ertan, 2017, 2018b), and CCOs (Benli & Ertan, 2018a) can be reproduced in the same long-term evolution model with very similar main disc parameters, supporting the idea proposed by Alpar (2001).

In this model, estimated magnetic dipole moments of these neutron star populations range from $\sim 10^{29}$ G cm^3 to a few 10^{30} G cm^3, which are well below the values inferred from the magnetic dipole torque formula. From the numerical simulations, most AXP/SGRs are estimated to be in the accretion regime, while XDINs are found in the strong propeller regime. In line with these results, it was shown that the characteristic high-energy spectra of AXPs can be produced in the accretion column, consistently with the observed phase dependent pulse profiles (Trümper et al., 2010, 2013; Kylafis, Trümper & Ertan, 2014).

In this work, we investigate the evolution of the rotating radio transient J1819 in the same model. We also try to understand the conditions responsible for the radio emis-

sion characteristics of RRATs through comparisons with the estimated properties of the other neutron star populations in the same model. In Section 2.2, we briefly describe our model and give the results of the numerical simulations for J1819. Our conclusions are summarized in Section 2.3.

2.2 The Model and Application to RRAT J1819–1458

Since the details of the model with applications to other neutron star systems are described in the earlier work (see e.g. Ertan et al., 2014; Benli & Ertan, 2016, 2017) here we summarize the initial conditions and the basic disc parameters. To clarify the estimation of the lower limits to the dipole field strengths of RRATs, we also briefly describe the torque calculation employed in the model.

In the fallback disc model, the rotational evolution of the neutron star is governed mainly by the evolution of the disc, irradiated by the X-rays, produced either by mass accretion onto the star or by intrinsic cooling of the star when accretion is not allowed. In the spin-down phase there are two basic states: (1) the accretion with spin-down (ASD) state, and (2) the propeller state. In the ASD state, the inner disc interacts with the dipole field of the star in an interaction region (boundary) between the conventional Alfvén radius, r_A, and the co-rotation radius, r_{co}, at which the field lines co-rotating with the star have the same speed as the Kepler speed of the disc matter. To calculate the magnetic spin-down torque acting on the star we integrate the magnetic torques from r_{co} to r_A taking $B_z \simeq B_\phi$, where B_z and B_ϕ are the poloidal and azimuthal components of the field lines interacting with the inner disc. That is, for the ASD phase, we assume that the inner radius of the boundary region is equal to r_{co}. The conventional Alfvén radius can be written as $r_A \simeq (GM)^{-1/7} \mu^{4/7} \dot{M}_{in}^{-2/7}$, where G is the gravitational constant, M and μ are the mass and the magnetic dipole moment of the neutron star. The integrated magnetic spin-down torque can be written in terms of the disc mass-flow rate, $\dot{M}_{in}$, as

$$N_{SD} = \frac{1}{2} \dot{M}_{in} (GMr_A)^{1/2} \left[1 - (r_A/r_{co})^3 \right] \tag{2.1}$$

(Ertan & Erkut, 2008). When the estimated r_A is greater than the light cylinder radius $r_{LC} = c/\Omega_*$, where c is the speed of light, we replace r_A in equation (2.1) with r_{LC}. In the

total torque calculation, we also include the magnetic dipole torque $N_{\mathrm{dip}} = -2\,\mu^2\Omega_*^3/3c^3$, where Ω_* is the angular frequency of the neutron star, and the spin-up torque resulting from the mass-flow onto the star in the ASD phase, $N_{\mathrm{SU}} \simeq \dot{M}_*(GMr_{\mathrm{co}})^{1/2}$, where $\dot{M}_*$ is the rate of mass accretion onto the star. We calculate the total torque as $N_{\mathrm{TOT}} = N_{\mathrm{SU}} + N_{\mathrm{dip}} + N_{\mathrm{SD}}$. Over the long-term evolution of AXP/SGRs and XDINs, N_{dip} and N_{SU} are usually negligible in comparison with N_{SD}.

Since the critical condition for transition to the propeller phase is not well known, we use the simplified condition $r_{\mathrm{A}} = r_{\mathrm{LC}}$ for the accretion-propeller transition. Recently, Ertan (2017) estimated the critical accretion rate, $\dot{M}_{\mathrm{crit}}$, for this transition which is consistent with the minimum accretion rates estimated for the transitional millisecond pulsars (tMSPs) (see e.g. Jaodand et al., 2016). The $\dot{M}_{\mathrm{crit}}$ estimated from the observations of tMSPs ($\sim 10^{13}$ g s^{-1}) are much lower than the rates corresponding to $r_{\mathrm{A}} = r_{\mathrm{co}}$, the critical condition for the onset of the propeller phase in the conventional models (Illarionov & Siuniaev, 1975). Our simplified propeller criterion is roughly in agreement with $\dot{M}_{\mathrm{crit}}$ estimated by Ertan (2017). In particular, for J1819, our results indicate that the source is currently in the accretion phase with $\dot{M}_{\mathrm{in}} \sim 2 \times 10^{13}$ g s$^{-1} > \dot{M}_{\mathrm{crit}} \approx 10^{12}$ g s^{-1} estimated with the model of Ertan (2017) for $P_0 = 300$ ms and $B_0 \simeq 4.6 \times 10^{11}$ G indicated by our model results (see below). Furthermore, since the onset of the propeller phase corresponds to sharp decay of L_{X}, the uncertainty in $\dot{M}_{\mathrm{crit}}$ does not affect the model curves significantly.

Starting from the outermost disc, the disc regions with effective temperature, T_{eff}, less than a critical temperature T_{P} becomes viscously passive. The dynamical outer disc radius r_{out} is calculated as $r_{\mathrm{out}} = r(T_{\mathrm{eff}} = T_{\mathrm{P}})$. In the long-term evolution, r_{out} decreases with decreasing X-ray irradiation flux that can be written as $F_{\mathrm{irr}} \simeq 1.2\,CL_{\mathrm{x}}/(\pi r^2)$ (Fukue, 1992), where r is radial distance from the star, L_{x} is the X-ray luminosity of the star, and C is the irradiation parameter which depends on the disc geometry and the albedo of the disc surfaces. Individual source properties of AXP/SGRs, XDINs, HBRPs, and CCOs could be reproduced self consistently with $T_{\mathrm{P}} \sim 50 - 150$ K (Benli & Ertan, 2016, 2017, 2018b,a) and $C \sim (1 - 7) \times 10^{-4}$ (Ertan & Çalışkan, 2006; Ertan et al., 2007). The T_{P} values estimated in our model are in agreement with results indicating that the disc is likely to be active at temperatures ~ 300 K (Inutsuka & Sano, 2005), while our C range is similar to that estimated for the low-mass X-ray binaries (see e.g. Dubus et al., 1999).

For the kinematic viscosity, we use the α-prescription, $\nu = \alpha \, c_\mathrm{s} \, h$ (Shakura & Sunyaev, 1973), where c_s is the sound speed, h is the pressure scale-height of the disc, and α is the kinematic viscosity parameter.

The main disc parameters, α, C, and T_P are similar for the fallback discs in different neutron star populations. The initial conditions, namely the strength of the magnetic dipole field on the pole of the star, B_0, the initial rotational period, P_0, and the initial mass of the disc, M_d, are mainly responsible for rather different characteristics emerging during the evolutionary phases of the sources. Through many simulations, we determine the allowed ranges of the initial conditions that can produce the P, $\dot{P}$, and L_x of sources simultaneously. In most cases, the long-term evolution is not sensitive to P_0 (see Ertan et al., 2009, for details). In the present case, we take $P_0 = 300$ ms, the center of the Gaussian distribution estimated for the initial periods of the radio pulsars (Faucher-Giguère & Kaspi, 2006). In Fig. 2.1, we give illustrative model curves that can represent the long-term evolution of J1819. We obtain these model curves with $T_\mathrm{P} = 53$ K, $C = (2 - 7) \times 10^{-4}$, and $\alpha = 0.045$, which are the typical values used in all earlier applications of the same model to AXP/SGR, XDINs and HBRPs (see e.g. Benli & Ertan, 2016). The illustrative sources in Fig. 2.1 reach the observed P, $\dot{P}$, and L_X of J1819 at an age of $\sim 2 \times 10^5$ yr, when the source is evolving in the accretion phase. The inner radius of the disc is more than 2 orders of magnitude greater than the radius of the star. That is, in the accretion phase the main source of the X-rays is the accretion onto the neutron star, while the contribution of the inner disc to the X-ray luminosity is negligible. The model constrains B_0 to a rather narrow range around $\sim 5 \times 10^{11}$ G, while the source properties can be reproduced with a large range of disc masses, M_d (see Fig. 2.1).

What is the basic, common property causing RRATs to produce radio bursts, and no regular radio pulsations? The dipole field strength indicated by the model results and the measured period place J1819 below and close to the pulsar death line in the $B_0 - P$ plane (Fig. 2.2). The model source is evolving into the properties of XDINs, which do not show RRAT behavior. It is not clear whether all RRATs are close to and below the pulsar death line. For RRATs other than J1819, for which the X-ray luminosity is not detected, it is not easy to pin down the evolutionary status with P and $\dot{P}$ alone. Nevertheless, we can estimate the lower bounds on B_0 ($B_{0,\mathrm{min}}$), for the sources with measured $\dot{P}$. In our model, the maximum spin-down torque is obtained in the accretion with spin-down (ASD)

phase when the source is not very close to rotational equilibrium. This corresponds to the constant $\dot{P}$ phase (see Fig. 2.1) over which the second (negative) term of the magnetic spin-down torque (equation 2.1) dominates both the accretion torque and the magnetic dipole torque. For this phase of evolution, it can be seen from equation (2.1) that the torque is independent of $\dot{M}_{\mathrm{in}}$, and the minimum dipole field strength on the pole of the star can be estimated as B_0 $(B_{0,\mathrm{min}}) \simeq 1.5 \, \dot{P}_{-11}^{1/2} \, 10^{12}$ G where $\dot{P}_{-11}^{1/2}$ is the period derivative in 10^{-11} s s^{-1}. This formula, which underestimates the B_0 values for the sources that are in the propeller phase or close to the rotational equilibrium in the accretion phase, gives the minimum possible field strength for a given $\dot{P}$ independently of $\dot{M}_{\mathrm{in}}$. These $B_{0,\mathrm{min}}$ values are plotted in Fig. 2.2.

Without X-ray luminosity information, we cannot estimate the actual field strength B_0. If the RRAT behavior of the sources start when they are close to the pulsar death line, the actual B_0 is likely to be between $B_{0,\mathrm{min}}$ and the B_0 corresponding to the period of the source on the pulsar death line. The estimated $B_{0,\mathrm{min}}$ values seen in Fig. 2.2 is important in that it is compatible with a continuous distribution for the B_0 values of all single neutron star populations (AXP/SGR, XDIN, HBRP, RRAT and CCO) in the fallback disc model, filling the gap between $B_0 \sim 10^9$ G for CCOs (Benli & Ertan, 2018a) and $B_0 \gtrsim 10^{11}$ G for the other populations (Alpar, 2001; Ekşi & Alpar, 2003; Ertan et al., 2007, 2009, 2014; Ertan, 2017; Benli & Ertan, 2017, 2018b).
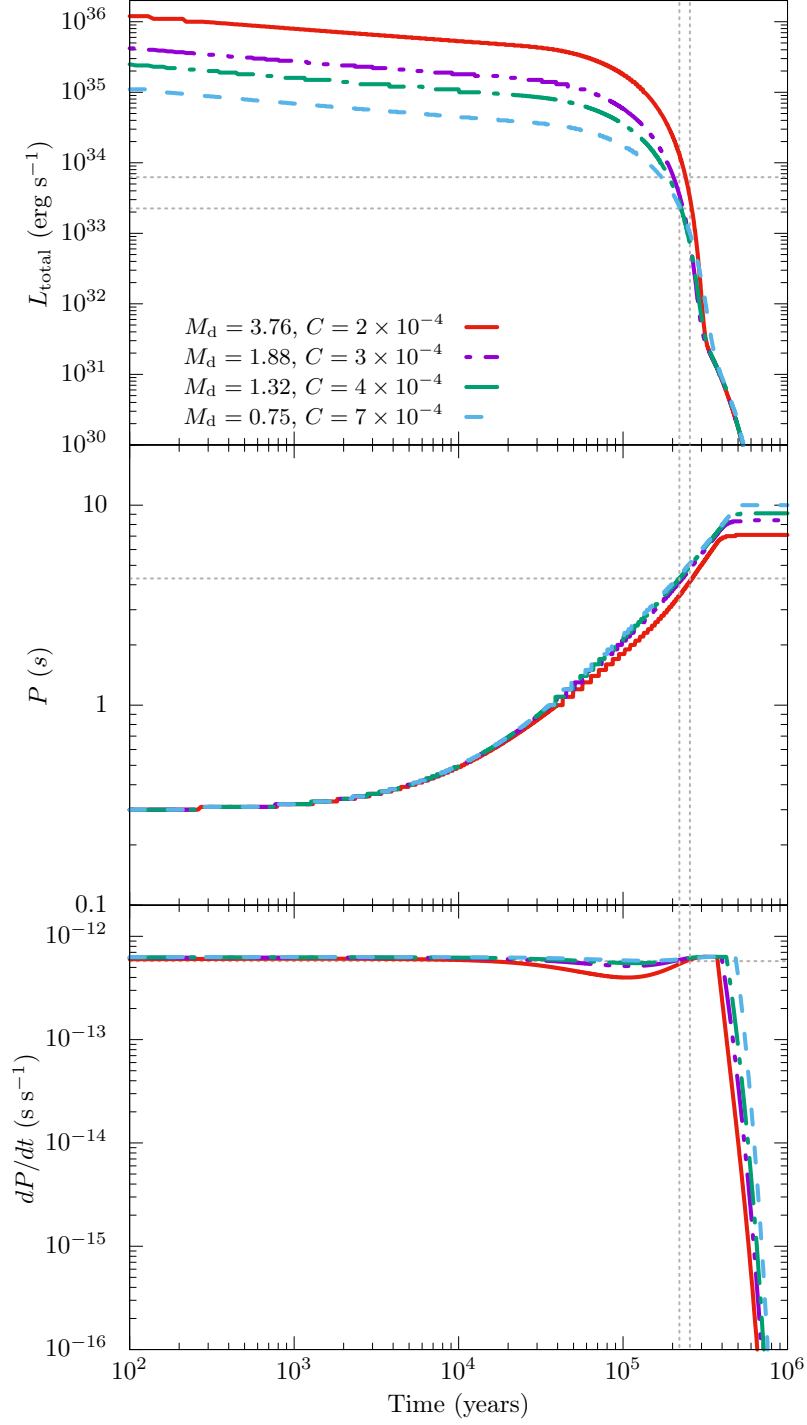
Figure 2.1: Illustrative model curves for the long-term evolution of the J1819–1458. These curves are obtained with $B_0 = 4.6 \times 10^{11}$ G. The values of M_d in units of 10^{-5} $M_\odot$ and C parameter are given in the top panel. The horizontal dotted lines show the observed $P = 4.26$ s, $\dot{P} \approx 5.75 \times 10^{-13}$ s s^{-1}, and $L_x = 4 \times 10^{33}$ $(d/3.6$ kpc$)^2$ erg s^{-1} with 25 % uncertainty (McLaughlin et al., 2006; Keane et al., 2011; Rea et al., 2009). For all these curves, $\alpha = 0.045$ and $T_P = 53$ K (see the text for details).

18
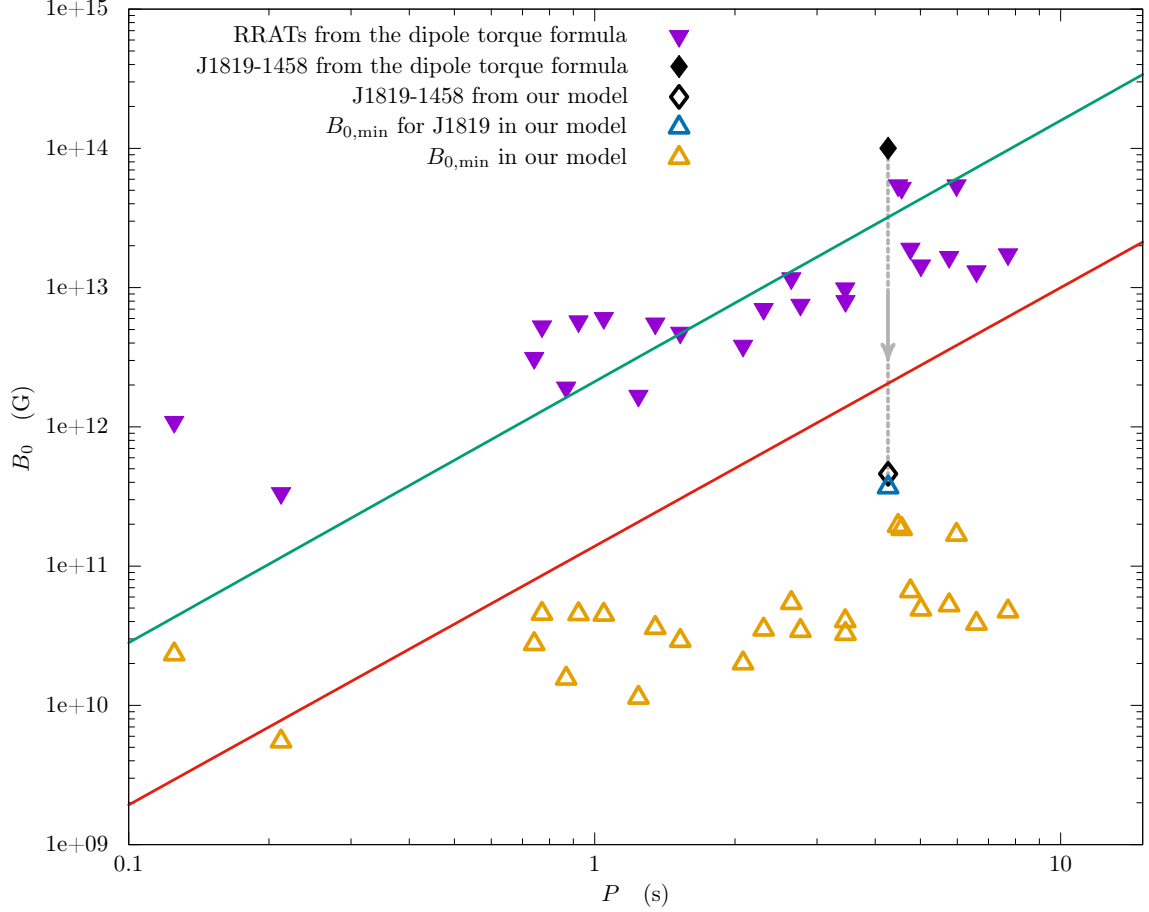
Figure 2.2: B_0 - P diagram. Filled and open diamonds show the B_0 values for J1819 inferred from the dipole torque formula ($\simeq 10^{14}$ G) and estimated in our model ($\simeq 4.6 \times 10^{11}$ G) respectively. The minimum B_0 ($B_{0,\min}$) values estimated in our model for the other RRATs with known P and $\dot{P}$ (McLaughlin et al., 2006; Deneva et al., 2009; Burke-Spolaor & Bailes, 2010; Keane et al., 2010, 2011; Burke-Spolaor et al., 2011) are marked with open triangles using $B_{0,\min} \simeq 1.5 \, \dot{P}_{-11}^{1/2} \, 10^{12}$ G (see the text). For each of these sources, B_0 inferred from the dipole torque formula are also plotted (inverse filled triangle). Solid lines represent the borders of the death valley (Chen & Ruderman, 1993). The lower border is similar to the classical pulsar death line (Bhattacharya et al., 1992).

2.3 Summary and Conclusion

We have investigated the long-term evolution of J1819–1458 which is the only RRAT detected in X-rays. We have shown that the period, period derivative and X-ray luminosity of the source can be explained in the same model that can account for the long-term evolutions of AXP/SGRs, XDINs, HBRPs, and CCOs. The model can reproduce the properties of the source only with a narrow range of B_0 around 4.6×10^{11} G, while reasonable model curves are obtained with rather different initial disc masses ($(0.75 - 3.76) \times 10^{-5} \ M_\odot$). The model sources reach the properties of J1819 in the accretion with spin-down (ASD) phase at an age $\sim 2 \times 10^5$ yr, when the estimated cooling luminosity of the neutron stars is a few per cent of the observed L_X of J1819. In the accretion phase, the mass-flow onto the neutron star is expected to switch off the radio pulses. Even if the accretion stops by some reason, we do not expect regular pulsed radio emission from J1819, since the B_0 indicated by our model and the measured P place the source below the pulsar death line.

Illustrative model curves in Fig. 2.1 imply that J1819 is currently evolving through lower part of the AXP/SGR region in the $P - \dot{P}$ diagram. Currently, the short-term timing behavior of the source seems to have been affected by the glitch effects (Bhattacharyya et al., 2018). From the model results, we estimate that J1819 will reach the XDIN properties within a few 10^5 yr (Fig. 2.1).

The illustrative model curves in Fig. 2.1 imply that the source is evolving into the XDIN properties. This result is not very sensitive to the initial period, the disc mass and the resultant L_X history of the source. For the other RRATs, since the X-ray luminosities are not known, it is not possible to estimate their evolutionary paths and the B_0 values. Nevertheless, the lower bound, $B_{0,\mathrm{min}}$ for a given source can be estimated using the most efficient torque reached in the ASD phase and the measured $\dot{P}$ of the source (Section 2.3). In Fig. 2.2, it is seen that these lower limits on B_0 allow a continuous B_0 distribution from CCOs to AXP/SGRs in the fallback disc model.

The estimated evolution of J1819 toward the XDIN population might indicate that all known XDINs could have evolved through RRAT phase in the past. The fact that all measured RRAT periods are smaller than 8 s, and that 4 out of 7 XDINs have periods greater than 8 s could point to a maximum period (for a given B_0) above which RRAT

behavior disappear. Considering that we have found J1819 below the death line, for a given source, there could be a certain RRAT phase that starts after the termination of the normal radio pulsations, and ends above a critical P for this particular neutron star. It is not clear whether the RRAT behavior itself is related to presence or properties of fallback disc around the source. We need further detections of RRATs in X-rays to test these ideas in depth through long-term evolutionary analysis of these sources.

Chapter 3

SUMMARY AND CONCLUSION

We have investigated the physical properties and the long-term evolution of RRATs in the fallback disc model. For more than 100 RRATs, periods are between 0.1 and 7 s. Period derivatives ($\sim 10^{-16} - 10^{-13}$ s s^{-1}) were measured for 29 sources (McLaughlin et al., 2006; Keane et al., 2011; Cui et al., 2017). Among these 100 RRATs, because of the uncertainties in their positions, the X-ray luminosity was estimated only for J1819–1458 ($L_{\mathrm{X}} = 4 \times 10^{33}$ ($d/3.6$ kpc)^2 erg s^{-1}; Rea et al., 2009), and there are upper limits for J0847–4316 and J1846–0257 (Kaplan et al., 2009). The fallback disc model employed in this thesis is the same model that was applied earlier to AXP/SGRs (Benli & Ertan, 2016), XDINs (Ertan et al., 2014), HBRPs (Benli & Ertan, 2017, 2018b) and CCOs (Benli & Ertan, 2018a). The rotational properties and the X-ray luminosities of the individual sources were successfully reproduced for all these systems using similar basic disc parameters, namely the irradiation efficiency (C), viscosity parameter (α), and the critical inactivation temperature of the disc (T_{P}). These parameters are expected to be similar for different systems within the simplification of the model, since the fallback discs of these systems are likely to have similar chemical compositions.

Results of the earlier applications of the model can be summarized as follows:

Most of the known AXP/SGRs are currently in the accretion phase. The two low-B-magnetars evolved in the accretion phase to long periods, completed the accretion phase, and are currently in the propeller phase. Their dipole field strengths are found to be $B_0 \simeq 10^{12} - 10^{13}$ G (Benli & Ertan, 2016). These sources can reach periods longer than present upper limit (~ 12 s) at late phases of evolution with X-ray luminosities likely to be detection limits.

Out of 7 XDINs, 6 sources with confirmed period derivatives have $B_0 \sim 10^{11} - 10^{12}$ G, lower than those of AXP/SGRs (Ertan et al., 2014; Ertan, 2017). These sources are found

in the propeller phase. These weak fields and long periods place them well below the radio-pulsar death line, in the $B_0 - P$ plane. That is, our model results indicate that the non-detection of radio pulses from XDINs is not due to beaming effect.

The properties of all known HBRPs (8 sources) are reproduced in the model in the propeller phase consistently with their radio-pulsar behavior. Their B_0 values are found in the $3 \times 10^{11} - 6 \times 10^{12}$ G range (Benli & Ertan, 2017, 2018b). Together with observed periods and these dipole fields, HBRPs are found to be sufficiently strong to produce pulsed radio emission. For 3 HBRPs, the second derivatives of the periods were also measured. The model sources can reach observed P, $\dot{P}$, $\ddot{P}$ and L_{X} simultaneously for these there sources (Benli & Ertan, 2017).

CCOs, which were detected at the centers of supernova remnants, are young sources with weak dipole fields. Even the dipole-torque formula gives $\sim 10^{10}$ G for the three CCOs with known P and $\dot{P}$. In our model, these sources are in the accretion phase with $B_0 \sim$ a few 10^9 G (Benli & Ertan, 2018a). Due to these weak fields, CCOs are likely to evolve in the spin-up regime in the early phases of their evolutions. It is remarkable that for the 3 CCOs observed L_{X} values are much greater than the theoretical cooling luminosities corresponding to thir supernova ages. In the model, the accretion luminosity can account for the observed L_{X} values consistently with the P and $\dot{P}$ values, and the estimated supernova ages of these sources (Benli & Ertan, 2018a).

In the earlier work summarized above, rather different properties of individual sources in different populations are produced as a result of the differences in the initial conditions (B_0, P_0, M_{d}). Model curves indicate that there could be evolutionary connections between these systems. For instance, a fraction of the HBRPs could be evolving towards the AXP/SGRs properties, while the remaining fraction is approaching the ordinary radio-pulsar properties. Some young XDINs, when they are still in the accretion phase, could be identified as AXP/SGRs.

In the present work, we have studied the long-term evolution of J1819, which is the only RRAT with measured L_{X}, in the fallback disc model. Our model results show that the rotational properties ($P = 4.26$ s and $\dot{P} \approx 5.75 \times 10^{-13}$ s s^{-1}) and the X-ray luminosity of J1819 can be acquired by a neutron star evolving with a fallback disc with the initial conditions $B_0 = 4.6 \times 10^{11}$ G, $M_{\mathrm{d}} = (0.75 - 3.76) \times 10^{-5} M_\odot$ and $P_0 = 300$ ms. These results are obtained with the disc parameters $C = (2 - 7) \times 10^{-4}$, $T_{\mathrm{P}} = 53$ K

and $\alpha = 0.045$. The model sources with different M_d values reaches the properties of J1819 and evolve towards XDIN properties at ages greater than a few 10^5 yr (see Fig. 2.1). Our results indicate that J1819 is currently in the accretion phase and powered by the accretion luminosity.

For AXP/SGRs, XDINs, and HBRPs, the B_0 values obtained from the model have a continuous distribution from $\sim 10^{11}$ G to 10^{13} G. There seems to be a gap between the B_0 values of CCOs (a few 10^9 G) and XDINs ($\gtrsim 10^{11}$ G). The only RRAT with estimated X-ray luminosity (J1819–1458) is not sufficient to test whether the RRAT population could fill this B_0 gap. Nevertheless, it is possible to estimate the minimum possible B_0 values, $B_{0,\mathrm{min}}$, for the RRATs, with unknown L_X, using the, measured P and $\dot{P}$ values. For 29 RRATs, we find that $B_{0,\mathrm{min}}$ values are in the range of $\sim 5 \times (10^9 - 10^{11})$ G, which allows an actual B_0 distribution that fill the B_0 gap between the field strengths of CCOs and XDINs.

Earlier work on XDINs show that the evolutionary model curves of XDINs pass through the properties of J1819–1458 (Ertan et al., 2014, Fig. 3), indicating that a fraction of RRATs could be progenitors of XDINs. Indeed, it can be seen from Fig. 2.1 that J1819–1458 is evolving towards the XDIN properties (see Fig. 1.2). We find J1819 below the pulsar death line in the $B_0 - P$ plane (see Fig. 2.2). The source is closer to the death line than XDINs are. This might be reason for the sporadic radio behavior of J1819. For a given B_0, the radio bursts could terminate at a certain P before the source becomes an XDIN, considering that XDINs do not show RRAT behavior. Out of 7 XDINs, 5 sources here $P > 7$ s while, the maximum P for more than 100 RRATs is about 7 s. This could be another implication of the evolutionary link between these systems. To understand the common properties of RRATs causing their sporadic radio bursts, we need detections of further sources in X-rays. This would allow us to investigate and compare their evolutionary phases in more detail. The evolutionary links between young neutron star populations will be the subject of our future work.
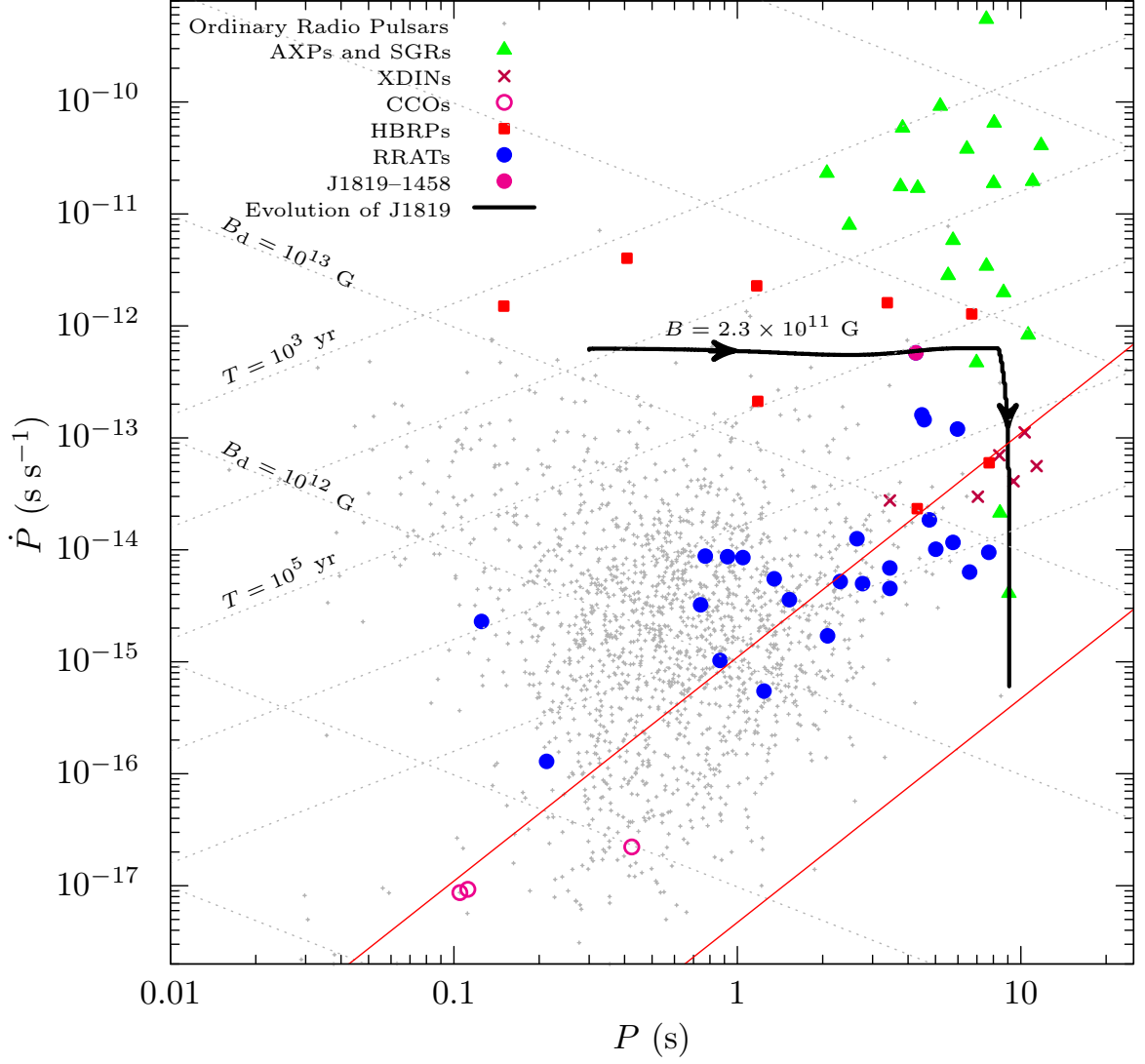
Figure 3.1: The long term evolution of J1819–1458 in the $P - \dot{P}$ diagram which contains the populations of AXP/SGRs, XDINs, HBRPs, CCOs and RRATs. Solid lines illustrate the borders of the death valley (Chen & Ruderman, 1993). The curve represents the evolutionary path of J1819-1458, which is the only RRAT with estimated L_X. The initial conditions set as $B_0 = 4.6 \times 10^{11}$ G, $M_d = 1.32 \times 10^{-5} M_\odot$, $P_0 = 300$ ms. The main disc parameters are taken as $C = 4 \times 10^{-4}$, $T_P = 53$ K and $\alpha = 0.045$. It is seen that J1819–1458 is evolving towards XDIN region. Indeed, the source arrives the XDIN region with L_X similar to those of XDINs (see also Fig. 2.1).

Bibliography

Abdo A. A. et al., 2013, ApJS, 208, 17

Alpar M. A., 2001, ApJ, 554, 1245

Alpar M. A., Cheng A. F., Ruderman M. A., Shaham J., 1982, Nature, 300, 728

Alpar M. A., Ertan Ü., Çalışkan Ş., 2011, ApJ, 732, L4

Baade W., Zwicky F., 1934, Physical Review, 46, 76

Benli O., Çalışkan Ş., Ertan Ü., Alpar M. A., Trümper J. E., Kylafis N. D., 2013, ApJ, 778, 119

Benli O., Ertan Ü., 2016, MNRAS, 457, 4114

Benli O., Ertan Ü., 2017, MNRAS, 471, 2553

Benli O., Ertan Ü., 2018a, MNRAS

Benli O., Ertan Ü., 2018b, Nature, 61, 78

Bhalerao V. et al., 2015, MNRAS, 447, 2274

Bhattacharya D., Wijers R. A. M. J., Hartman J. W., Verbunt F., 1992, A&A, 254, 198

Bhattacharyya B. et al., 2018, MNRAS, 477, 4090

Bondi H., Hoyle F., 1944, MNRAS, 104, 273

Burderi L., D'Amico N., 1997, ApJ, 490, 343

Burderi L., King A. R., Wynn G. A., 1996, MNRAS, 283, L63

Burke-Spolaor S., Bailes M., 2010, MNRAS, 402, 855

Burke-Spolaor S. et al., 2011, MNRAS, 416, 2465

Çalışkan Ş., Ertan Ü., Alpar M. A., Trümper J. E., Kylafis N. D., 2013, MNRAS, 431, 1136

Cameron A. G. W., 1959, ApJ, 130, 916

Chadwick J., 1932, Nature, 129

Chatterjee P., Hernquist L., Narayan R., 2000, ApJ, 534, 373

Chen K., Ruderman M., 1993, ApJ, 402, 264

Chevalier R. A., 1989, ApJ, 346, 847

Colgate S. A., 1971, ApJ, 163, 221

Cui B.-Y., Boyles J., McLaughlin M. A., Palliyaguru N., 2017, ApJ, 840, 5

Davidson K., Ostriker J. P., 1973, ApJ, 179, 585

Deneva J. S. et al., 2009, ApJ, 703, 2259

Ding K. Y., Cheng K. S., Chau H. F., 1993, ApJ, 408, 167

Dubus G., Lasota J.-P., Hameury J.-M., Charles P., 1999, MNRAS, 303, 139

Duncan R. C., Thompson C., 1992, ApJ, 392, L9

Ekşi K. Y., Alpar M. A., 2003, ApJ, 599, 450

Ertan Ü., 2017, MNRAS, 466, 175

Ertan Ü., Alpar M. A., Erkut M. H., Ekşi K. Y., Çalışkan Ş., 2007, Ap&SS, 308, 73

Ertan Ü., Çalışkan Ş., 2006, ApJ, 649, L87

Ertan Ü., Çalışkan Ş., Benli O., Alpar M. A., 2014, MNRAS, 444, 1559

Ertan Ü., Ekşi K. Y., Erkut M. H., Alpar M. A., 2009, ApJ, 702, 1309

Ertan Ü., Erkut M. H., 2008, ApJ, 673, 1062

Faucher-Giguère C.-A., Kaspi V. M., 2006, ApJ, 643, 332

Fukue J., 1992, PASJ, 44, 663

Gavriil F. P., Gonzalez M. E., Gotthelf E. V., Kaspi V. M., Livingstone M. A., Woods P. M., 2008, Science, 319, 1802

Giacconi R., Gursky H., Paolini F. R., Rossi B. B., 1962, Physical Review Letters, 9, 439

Gold T., 1968, Nature, 218, 731

Gotthelf E. V., Halpern J. P., Alford J., 2013, ApJ, 765, 58

Haberl F., Motch C., Buckley D. A. H., Zickgraf F.-J., Pietsch W., 1997, A&A, 326, 662

Halpern J. P., Gotthelf E. V., 2010, ApJ, 709, 436

Hessels J. W. T., Ransom S. M., Stairs I. H., Freire P. C. C., Kaspi V. M., Camilo F., 2006, Science, 311, 1901

Hewish A., Bell S. J., Pilkington J. D. H., Scott P. F., Collins R. A., 1968, Nature, 217, 709

Hurley K. et al., 1999, Nature, 397, 41

Illarionov A. F., Siuniaev R. A., 1975, Soviet Astronomy Letters, 1, 73

Inutsuka S.-i., Sano T., 2005, ApJ, 628, L155

Israel G. L., Campana S., Dall'Osso S., Muno M. P., Cummings J., Perna R., Stella L., 2007, ApJ, 664, 448

Jahan Miri M., Bhattacharya D., 1994, MNRAS, 269, 455

Jaodand A., Archibald A. M., Hessels J. W. T., Bogdanov S., D'Angelo C. R., Patruno A., Bassa C., Deller A. T., 2016, ApJ, 830, 122

Kaplan D. L., Esposito P., Chatterjee S., Possenti A., McLaughlin M. A., Camilo F., Chakrabarty D., Slane P. O., 2009, MNRAS, 400, 1445

Kaspi V. M., 2010, Proceedings of the National Academy of Science, 107, 7147

Kaspi V. M., Gavriil F. P., Woods P. M., Jensen J. B., Roberts M. S. E., Chakrabarty D., 2003, ApJL, 588, L93

Keane E. F., Kramer M., 2008, MNRAS, 391, 2009

Keane E. F., Kramer M., Lyne A. G., Stappers B. W., McLaughlin M. A., 2011, MNRAS, 415, 3065

Keane E. F., Ludovici D. A., Eatough R. P., Kramer M., Lyne A. G., McLaughlin M. A., Stappers B. W., 2010, MNRAS, 401, 1057

Knight H. S., Bailes M., Manchester R. N., Ord S. M., Jacoby B. A., 2006, ApJ, 640, 941

Konar S., Bhattacharya D., 1997, MNRAS, 284, 311

Konar S., Bhattacharya D., 1999, MNRAS, 303, 588

Kylafis N. D., Trümper J. E., Ertan Ü., 2014, A&A, 562, A62

Lewin W. H. G., van Paradijs J., van den Heuvel E. P. J., 1995, Cambridge Astrophysics Series, 26

Livingstone M. A., Scholz P., Kaspi V. M., Ng C.-Y., Gavriil F. P., 2011, ApJL, 743, L38

Manchester R. N. et al., 2001, MNRAS, 328, 17

Mazets E. P., Golenetskij S. V., Guryan Y. A., 1979, Soviet Astronomy Letters, 5, 641

Mazets E. P., Golentskii S. V., Ilinskii V. N., Aptekar R. L., Guryan I. A., 1979, Nature, 282, 587

McLaughlin M. A. et al., 2009, MNRAS, 400, 1431

McLaughlin M. A. et al., 2006, Nature, 439, 817

McLaughlin M. A. et al., 2007, ApJ, 670, 1307

Mereghetti S., 2013, Brazilian Journal of Physics, 43, 356

Michel F. C., Dessler A. J., 1981, ApJ, 251, 654

Olausen S. A., Kaspi V. M., 2014, ApJs, 212, 6

Oppenheimer J. R., Volkoff G. M., 1939, Physical Review, 55, 374

Pacini F., 1967, Nature, 216, 567

Palmer D. M. et al., 2005, Nature, 434, 1107

Pavlov G. G., Kargaltsev O. Y., Sanwal D., Garmire G. P., 2001, ApJL, 554, L189

Popov S. B., Turolla R., Possenti A., 2006, MNRAS, 369, L23

Pringle J. E., Rees M. J., 1972, A&A, 21, 1

Radhakrishnan V., Srinivasan G., 1982, Current Science, 51, 1096

Rea N. et al., 2012, ApJ, 754, 27

Rea N. et al., 2009, ApJ, 703, L41

Redman S. L., Rankin J. M., 2009, MNRAS, 395, 1529

Ruderman M., Zhu T., Chen K., 1998, ApJ, 492, 267

Shakura N. I., Sunyaev R. A., 1973, A&A, 24, 337

Shklovsky I. S., 1967, ApJ, 148, L1

Srinivasan G., Bhattacharya D., Muslimov A. G., Tsygan A. J., 1990, Current Science, 59, 31

Taylor G. B., Stovall K., McCrackan M., McLaughlin M. A., Miller R., Karako-Argaman C., Dowell J., Schinzel F. K., 2016, ApJ, 831, 140

Thompson C., Duncan R. C., 1995, MNRAS, 275, 255

Tolman R. C., 1939, Physical Review, 55, 364

Trümper J. E., Dennerl K., Kylafis N. D., Ertan Ü., Zezas A., 2013, ApJ, 764, 49

Trümper J. E., Zezas A., Ertan Ü., Kylafis N. D., 2010, A&A, 518, A46

Turolla R., 2009, in Astrophysics and Space Science Library, Vol. 357, Astrophysics and Space Science Library, Becker W., ed., p. 141

van den Heuvel E. P. J., Heise J., 1972, Nature Physical Science, 239, 67

Weltevrede P., Stappers B. W., Rankin J. M., Wright G. A. E., 2006, ApJ, 645, L149

White N. E., 2002, High-mass X-ray binaries. Kluwer Academic Publishers, p. 823

Younes G., Kouveliotou C., Roberts O., 2016, GRB Coordinates Network, Circular Service, No. 19736, #1 (2016), 19736

Young M. D., Manchester R. N., Johnston S., 1999, Nature, 400, 848

Zhang B., Gil J., Dyks J., 2007, MNRAS, 374, 1103